Spectrum of Engineering Sciences
ISSN (e) 3007-3138 (p) 3007-312X
Volume 4, Issue 2, 2026

ACUTE LYMPHOBLASTIC LEUKEMIA SUBTYPE CLASSIFICATION USING CONVOLUTIONAL NEURAL NETWORKS ON PERIPHERAL BLOOD SMEAR IMAGE

Muhammad Idrees[1]*, Shahab Khan[2], Muhammad Sultan Ismail[3], Muhammad Saleem[4], Ashfaq Ahmad[5], Hamza Javed[6], Zafar Iqbal[7], Muneeba Islam[8]

*[*1]Computer Science Department, University of Chakwal, Pakistan*
[2]MS Scholar, Computer Science Department, MY University Islamabad, Pakistan
[3]Jinnah college of Commerce & Technology, Bahawalpur, Pakistan
[4]Lecturer, Computer Science Department, MY University Islamabad, Pakistan
[5]Assistant Professor, Computer Science Department, MY University Islamabad, Pakistan
[6]Lecturer, Computer Science Department, IQRA University H-9 Islamabad, Pakistan
[7]Lecturer, Computer Science Department, MY University Islamabad, Pakistan
[8]Lecturer, Computer Science Department, MY University Islamabad, Pakistan

DOI:

Keywords:
Acute Lymphoblastic Leukemia, Convolutional Neural Networks, Blood Smear Classification, Deep Learning, Automated Diagnosis

Article History
Received on 10 Jan, 2026
Accepted on 05 Feb, 2026
Published on 07 Feb, 2026

Corresponding Author: Muhammad Idrees

Abstract

Lymphoblastic Leukemia (ALL) is the most common kind of cancer in children. It is caused by too many immature lymphoblasts growing in the bone marrow. Accurate subtype identification is crucial for timely and effective treatment. This work presents a deep learning approach for the automated classification of four diagnostic categories based on microscopic peripheral blood smear images: benign (hematogones) and three malignant subtypes of acute lymphoblastic leukemia (Early Pre-B, Pre-B, and Pro-B). Transfer learning was used to improve four pre-trained convolutional neural network architectures EfficientNet-B3, VGG16, DenseNet-121, and ResNet-50–on a dataset of 3,256 images. EfficientNet-B3 achieved the highest test accuracy of 98.57%, followed by VGG16 (98.37%), DenseNet-121 (97.76%), and ResNet-50 (95.92%). The proposed strategy demonstrates enhanced diagnostic precision and has considerable potential to reduce observer variability, minimize diagnostic errors, and expedite clinical decision-making in all screening and subtype identification processes

1 Introduction

Acute Lymphoblastic Leukemia (ALL) is a malignant hematological disorder mostly affecting children and represents a considerable public health concern due to its potentially fatal outcomes if not promptly identified and treated [2, 4, 9, 14]. The disorder arises from the uncontrolled proliferation of immature white blood cells (lymphoblasts) in the bone marrow, obstructing normal hematopoiesis and leading to symptoms such as fatigue, recurrent infections, and bleeding [2, 9]. Acute Lymphoblastic Leukemia (ALL) is classified into two primary categories: benign hematogones and malignant lymphoblasts. The malignant lymphoblasts are further categorized into Early Pre-B, Pre-B, and Pro-B subtypes. It is very important to know exactly what subtype it is since treatment choices and prognosis vary accordingly [7, 8]. The traditional way of diagnosing is to look at photographs of peripheral blood smears (PBS) by hand. This approach is subjective, time-consuming, and requires specialist knowledge, and little differences in shape make it more likely that the diagnosis will be wrong. [5,10]. Ali et al. proposed iAFP-ET, an Extra Tree Classifier model, to find anti- fungal peptides. In the model shown that how useful it is for mixed feature extraction.[17].

This study used a dataset of 3,256 PBS images sourced from 89 suspected ALL patients in Tehran, Iran [11]. The collection contains 504 benign shots and 2,752 malignant images, which are divided into three groups: Early Pre-B, Pre-B, and Pro-B. A hematological expert verified all the labels using flow cytometry [11]. Shamas et al. (Year) identified that a deep transfer learning model using VGG16 could precisely detect fifteen distinct lung diseases from chest X-rays. Convolutional neural network (CNN) architectures are versatile for automating intricate illness categorization from medical pictures [18].HSV-based segmentation was utilized to prepare the images such that lymphoblasts could be seen well. A major issue with the collection is that there aren't enough benign examples, which leads to class imbalance. We propose that a deep learning system that can automatically sort all subtypes using ImageNet-pretrained CNN models including EfficientNet-B3, VGG16, DenseNet-121, and ResNet-50. EfficientNet-B3 achieved the highest accuracy (98.57%), followed by VGG16 (98.37%), DenseNet-121 (97.76%), and ResNet-50 (95.92%). Images were resized, normalized, and augmented, while class weighting and regularization were applied to im- prove generalization and reduce bias toward majority classes. Compared with previously reported methods, which typically achieve 70–95% accuracy [10, 12, 15], the proposed system delivers superior performance without reliance on computationally expensive ensemble models, supporting its suitability for clinical use.

Early and accurate detection of Acute Lymphoblastic Leukemia (ALL) from peripheral blood smear (PBS) images has increasingly benefited from deep learning–based automated analysis systems. Convolutional neural networks (CNNs) and transfer learning approaches have demonstrated strong potential for both binary leukemia detection and multiclass subtype classification.

Pathan et al. [1] developed a CNN-based framework using a fine-tuned VGG16 model on 3,256 smear images for three ALL subtypes and benign cells, achieving 85% accuracy.

Despite promising results, the small dataset limited generalizability. Haque et al. [2] further enhanced detection performance by integrating preprocessing with transfer learning. Their Modified High-Boosting filtering technique combined with Inception–ResNet delivered F1-scores above 95% on both binary and multiclass datasets, though external validation was recommended due to dataset bias.

Several studies have applied ensemble and attention-based architectures. Bhute et al. [3] trained VGG16, ResNet50, and InceptionV3 models on the Raabin Leukemia dataset and reported up to 99.8% accuracy using an ensemble approach, albeit with high computational cost.

Ullah et al. [4] incorporated Efficient Channel Attention into VGG16 on the C-NMC dataset, improving detection accuracy to 91.1% and demonstrating the benefit of adaptive feature weighting. There have also been concepts for personalized CNN designs. Sampathila et al. released their description of the ALL-NET model at the reference number 5. The fact that it was trained on a better version of the C-NMC dataset and had classification accuracies close to 95% shows that lightweight convolutional neural networks (CNNs) may be deployed in clinical settings. Also, Mondal et al. [6] showed how ensemble learning may make systems more stable. They employed a weighted ensemble of five transfer-learning models and got an F1-score of 89.72% and an area under the curve (AUC) of 94.8%.

Other methods include subject-wise validation, hybrid deep learning pipelines, and analysis that is made better by segmentation. All of these are instances of methodology. Rezayi et al. performed tests that demonstrated the evaluation of lightweight CNNs, namely ResNet50 and VGG16, utilizing a competitive dataset. After using pre-trained weights, the results indicated an improvement in generalization, achieving an accuracy of 84.6%. Syed et al. [8] developed hierarchical classifiers to tell the difference between acute and chronic leukemia kinds, and they got an F1-score of 0.94. This was done even though it was still hard to categorize subtypes in detail because of their comparable shapes. Deep learning and improved feature extraction have shown promise in recent research for use in biological categorization. Models such as AIPs-SnTCN. [20] and Deep-AntiFP [21] use specialized neural networks and feature fusion to provide peptide and protein predictions with a high degree of accuracy. The importance of combining evolutionary and physicochemical variables for strong classification is further shown by an SVM-based predictor [22] and the iAFPs-EnC-GA ensemble [23]. The creation of more comprehensive frameworks for hematological image analysis has also improved the process of automatically identifying leukemia. Zhou et al. [9] achieved an accuracy rate of 89% in identifying ALL by the analysis of bone marrow smear pictures obtained from youngsters. A multi-stage CNN pipeline was used to do this. Almadhor et al. [10] achieved a 90% SVM-based accuracy on the C-NMC dataset by the integration of deep feature extraction with traditional machine-learning classifiers. This was done by combining the two ways. Ghulam et al. et al. [19] used a 2D Convolutional Neural Network (ACP-2DCNN), showing how CNN architectures may comprehend complicated, high- dimensional biological patterns useful for medical research. Park et al. [12] say that using EfficientNet-based white blood cell subtype categorization led to an accuracy rate of 88.6% when telling the difference between AML and ALL. This was a thorough look at all twelve different kinds of cells involved. The study's results show that CNN-based systems can reliably diagnose leukemia provided they have enough data, augmentation, and ensemble or attention-based methods. Nonetheless, significant challenges persist, including dataset imbalance, morphological similarity across classes, insufficient external validation, and suboptimal performance in multiclass scenarios. These constraints underscore the need for

Ongoing study into the advancement of novel designs and training approaches to accurately classify all subtypes inside healthcare organizations.

The main contributions of this research include:

- optimized preprocessing and HSV-based enhancement to improve cell visibility;
- handling of dataset imbalance through augmentation and weighted learning;
- evaluation of multiple deep learning architectures for ALL subtype classification; and
- Comprehensive comparison with existing approaches to demonstrate clinical relevance.

The remainder of this paper is organized as follows: Section 2 describes the dataset and methodology; Section 3 presents the results; Section 4 concludes the study; and lists the references.

2 Material and Methods

2.1 Dataset

The research used a publicly accessible dataset of 3,256 pictures of peripheral blood smears (PBS) from 89 people. After standard hematological staining, all samples were preserved in JPG format and obtained at a magnification of 100× the microscope. Hematopathology experts looked over and validated all of the photos using flow cytometry, which made sure that the diagnosis was quite reliable.

The dataset comprises four diagnostic categories:

- Benign (hematogones)
- Early Pre-B Acute Lymphoblastic Leukemia (ALL)
- Pre-B Acute Lymphoblastic Leukemia (ALL)
- Pro-B Acute Lymphoblastic Leukemia (ALL)

images, with benign samples representing the minority class.

2.2 Dataset Composition

Table 1 summarizes the distribution of the four diagnostic classes. The dataset contains 3,256

Table 1: ***Dataset Composition***

Class	Images	Percentage
Benign	504	15.5%
Early Pre-B	985	30.2%
Pre-B	963	29.6%
Pro-B	804	24.7%
Total	**3256**	**100%**

Stratified sampling was utilized to divide the data into three groups: training, valida- tion, and testing. The proportions of each class stayed the same. The table shows what happened after the division. 2.

Table 2: ***Dataset Split***

Subset	Total Images	Benign	Early Pre-B	Pre-B	Pro-B
Training (70%)	2276	352	689	673	562
Validation (15%)	490	76	148	145	121
Test (15%)	490	76	148	145	121
Total	**3256**	**504**	**985**	**963**	**804**

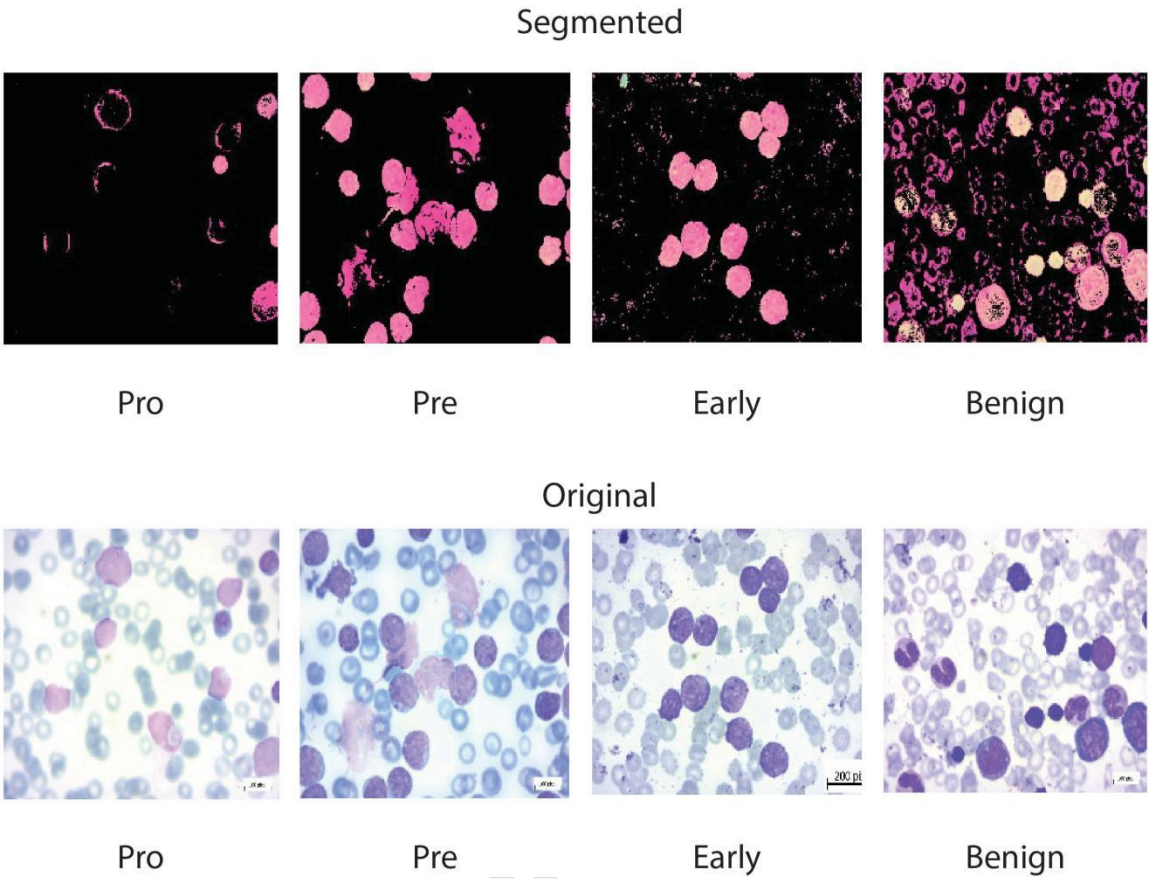

Figure 1: Class-Wise Examples of Peripheral Blood Smear Images for ALL Subtype Classification

2.3 Image Pre-Processing

All images were resized to 224 × 224 pixels and pixel intensities were normalized to the range [0,1] using a 1/255 scaling factor. By making sure that all samples had the same feature representation, this standardization made sure that it would operate with diverse convolutional neural network (CNN) designs and kept the training process steady. Because of this, preprocessing made the model more accurate and made sure that the leukemia groups were accurately grouped.

2.4 Data Augmentation

Data augmentation was applied exclusively to the training set to improve model gener- alization and mitigate class imbalance. The validation and test sets were subjected only to rescaling in order to preserve their original distributions. Augmentation operations included geometric and photometric transformations such as rotation, translation, shear, zoom, horizontal and vertical flipping, and brightness adjustment. Table 3 summarizes the augmentation parameters used for each model.

Table 3: *Data Augmentation Parameters for Different Models*

Model	Rotation	Shift (W/H)	Shear	Zoom	Flips	Brightness Range	Fill Mode
VGG16	≤40°	≤40%	≤40%	≤40%	H/V	0.5–1.5	Nearest
EfficientNet-B3	≤8°	≤8%	≤8%	≤8%	H/V	0.95–1.05	Nearest
DenseNet-121	≤8°	≤8%	≤8%	≤8%	H/V	0.95–1.05	Nearest
ResNet-50	≤8°	≤8%	≤8%	≤8%	H/V	0.95–1.05	Nearest

2.5 Feature Extraction

Four pretrained convolutional neural network (CNN) architectures—EfficientNet-B3, VGG16, DenseNet-121, and ResNet-50—were employed as feature extractors to learn discrimina- tive representations from peripheral blood smear images. All networks were initialized with ImageNet pretrained weights to leverage transfer learning and improve convergence
on the limited medical dataset.

Input images were resized to 224 × 224 × 3 and propagated through the convolutional layers of each model to generate high-level feature maps representing morphological char- acteristics of leukemic and benign lymphoid cells. EfficientNet-B3 produced feature maps of size 7×7×1536, VGG16 generated 7×7×512 maps, DenseNet-121 yielded 7×7×1024,
and ResNet-50 extracted 7 × 7 × 2048 representations.

These feature maps were subsequently flattened and passed to task-specific classifica- tion heads to perform multiclass ALL subtype prediction.

*All parameters fine-tuned in Phase 2

2.6 Optimizers and Hyper parameters

The models were trained using either the Adam optimizer or stochastic gradient descent (SGD), with learning rates selected separately for the two training phases, as summarized in Table 5. Adam was employed for EfficientNet-B3 and VGG16, while SGD with a momentum factor of 0.9 was applied to DenseNet-121 and ResNet-50. Dropout regularization in the range of 0.60 to 0.70 was incorporated intothe classification heads to mitigate overfitting, and additional fine-tuning dropout was applied to EfficientNet-B3. The sample size of 32 was kept the same for all experiments. We used a Tesla T4 GPU on Google Colab for all of our training. This made it easy to quickly analyze massive amounts of images and improve our models.

Table 4: *Model Architectures and Training Parameters*

Model	Total Parameters	Trainable (Phase 1)	Trainable (Phase 2)	Epochs/ Phase
EfficientNet-B3	12,365,619	1,581,056	12,365,619*	15 + 15
VGG16	15,248,196	533,508	15,248,196*	15 + 15
DenseNet-121	8,095,300	1,056,768	3,033,988	20 + 20
ResNet-50	25,694,084	2,105,344	24,302,596	20 + 20

Table 5: *Training Configuration and Hyperparameters*

Model	Optimizer	LR (P1)	LR (P2)	Momentum	Dropout
EfficientNet-B3	Adam	1×10^{-4}	1×10^{-5}	–	0.60
VGG16	Adam	5×10^{-6}	5×10^{-6}	–	0.70
DenseNet-121	SGD	3×10^{-4}	3×10^{-4}	0.9	0.60
ResNet-50	SGD	3×10^{-4}	3×10^{-4}	0.9	0.60

3 Results and Discussion

We utilized 490 photos of peripheral blood smears to evaluate four convolutional neural network models: EfficientNet-B3, VGG16, DenseNet-121, and ResNet-50. We then put the photographs into four groups: (benign, early pre-B, pre-B, and pro-B).

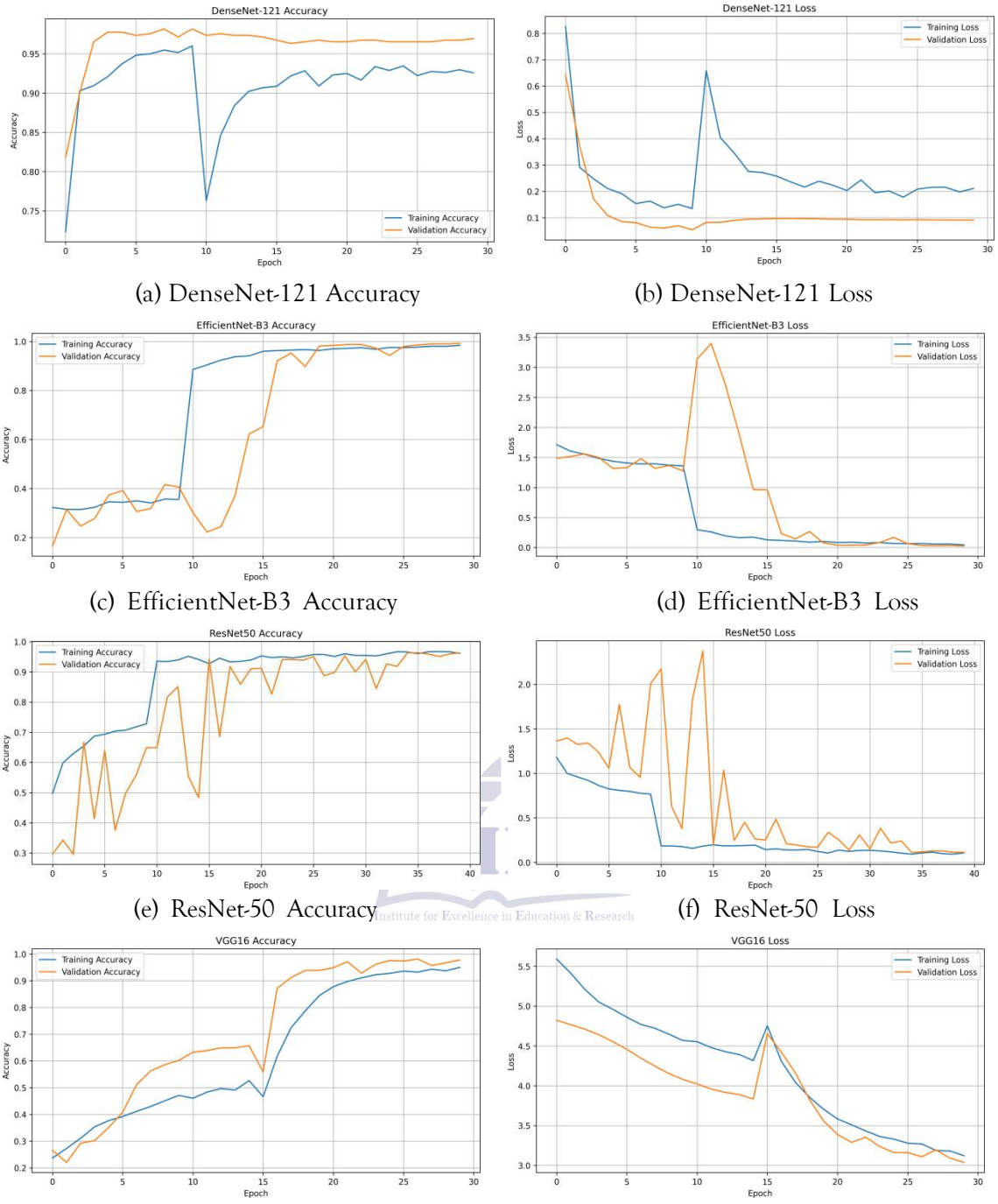

(a) DenseNet-121 Accuracy (b) DenseNet-121 Loss

(c) EfficientNet-B3 Accuracy (d) EfficientNet-B3 Loss

(e) ResNet-50 Accuracy (f) ResNet-50 Loss

(g) VGG16 Accuracy (h) VGG16 Loss

Figure 2: Training accuracy and loss curves for the four CNN architectures: DenseNet- 121 (a-b), *EfficientNet-B3 (c-d), ResNet-50 (e-f), and VGG16 (g-h).*

Table 6: ***Test Accuracy And Per-Class Precision, Recall, And f1-Score***

Model	Accuracy (%)	Class	Precision	Recall	F1-score
EfficientNet-B3	98.57	Benign	0.99	1.00	0.99
VGG16	98.37	Early Pre-B	0.99	0.99	0.99
DenseNet-121	97.76	Pre-B	0.99	0.98	0.98
		Pro-B	0.98	0.98	0.98

Benign	0.99	0.93	0.96
Early Pre-B	0.96	1.00	0.98
Pre-B	1.00	0.98	0.99
Pro-B	0.99	1.00	1.00
Benign	0.95	0.96	0.95
Pre-B	1.00	0.95	0.98

3.1 Training and Validation Curves

Figure 2 For each of the four models, show the accuracy and loss curves for training and validation. EfficientNet-B3 quickly reaches a level of accuracy that is good for training; it gets close to 1.0 quickly and stays above 0.98 by epoch 15. The loss curves go down consistently with minimal variation, which means that the model is good at generalizing and doesn't overfit, which is consistent with its best test accuracy of 98.57 VGG16's training accuracy quickly rises to 1.0, while its validation accuracy steadily rises to roughly 0.98. Validation accuracy drops a little between epochs 12 and 15, maybe because of active augmentation and high dropout rates. Still, the model gets close to ultimate alignment and does well on tests (98.37±. At first, DenseNet-121 gets virtually perfect training accuracy. Validation accuracy and loss, on the other hand, change a lot, especially between epochs 10 and 15. This instability shows that there is some overfitting, which lowers the test accuracy to 97.76. ResNet-50's validation accuracy and loss go from 0.85 to 0.98 during 40 epochs, even while its training accuracy reaches 1.0. The ongoing divergence shows that convergence is not working well and implies overfitting, which is in line with the model's lowest test accuracy of 95.72 In short, EfficientNet-B3 and VGG16 have the most stable training dynamics and the best ability to generalize. On the other hand, DenseNet-121 and ResNet-50 are not as stable.

3.2 Confusion Matrices

Figure 3a–3d present the confusion matrices for the four models on the test set.

EfficientNet-B3 shows the strongest performance with only seven misclassifications total (one to two per class) and perfect or near-perfect diagonal counts (Benign: 72, Early Pre-B: 142, Pre-B: 141, Pro-B: 117). The minor errors are distributed without clear patterns of systematic confusion between specific subtypes.

VGG16 performs nearly as well, with nine total errors—primarily minor confusions involving the Benign (five misclassified) and malignant classes, but zero errors in several cells, indicating robust separation of Early Pre-B, Pre-B, and Pro-B.

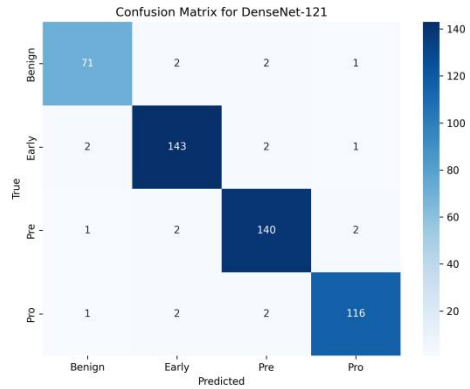

(a) DenseNet-121

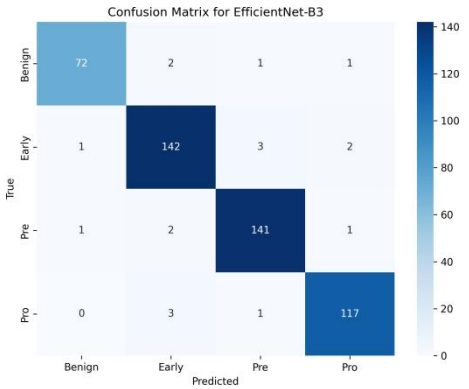

(b) EfficientNet-B3

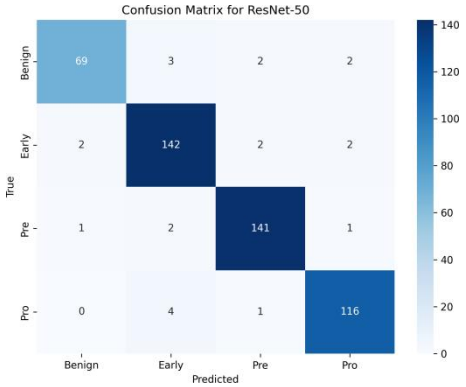

(c) ResNet-50

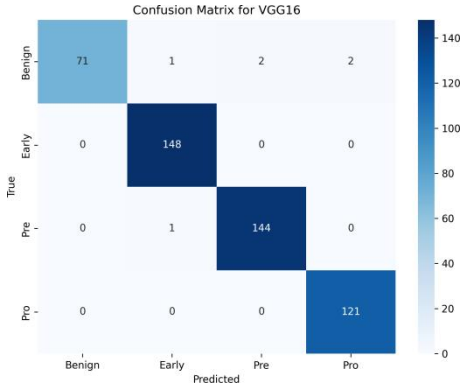

(d) VGG16

Figure 3: Confusion matrices for the four CNN models on the test set (490 images): (a) DenseNet-121, (b) EfficientNet-B3, (c) ResNet-50, and (d) VGG16. EfficientNet-B3 and VGG16 show near-perfect diagonal dominance with minimal misclassifications

DenseNet-121 and ResNet-50 display more scattered errors (approximately 15–20 misclassifications each). Both struggle most with the Benign class (five to seven misclassifications) and show occasional confusion between malignant subtypes (e.g., Early Pre-B misclassified as Pre-B or Pro-B). These patterns align with their lower overall accuracies (97.76% and 95.92%, respectively).

The near-diagonal dominance across all matrices, particularly for EfficientNet-B3 and VGG16, confirms effective discrimination of subtle morphological differences among ALL subtypes and benign hematogones.

3.3 Bar Graphs

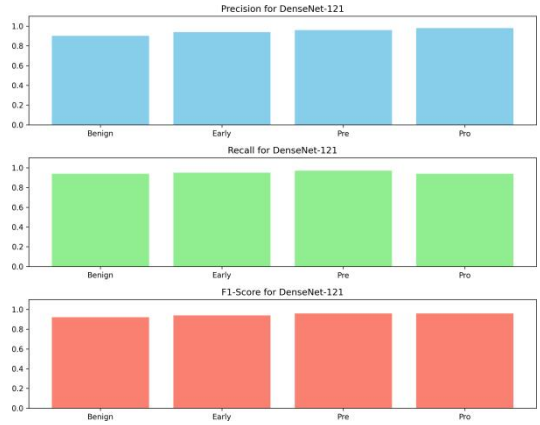

(a) DenseNet-121

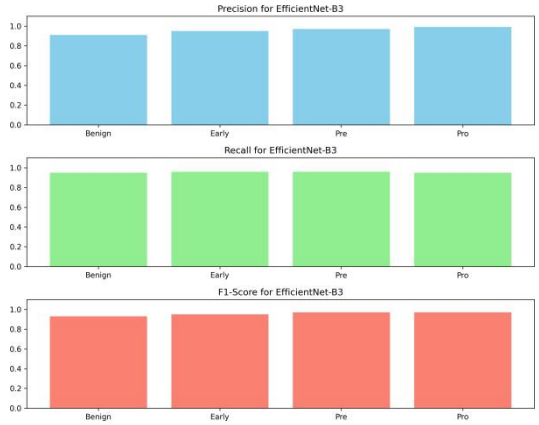

(b) EfficientNet-B3

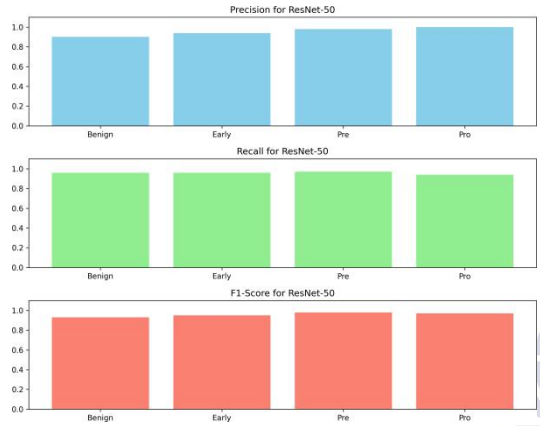

(c) ResNet-50

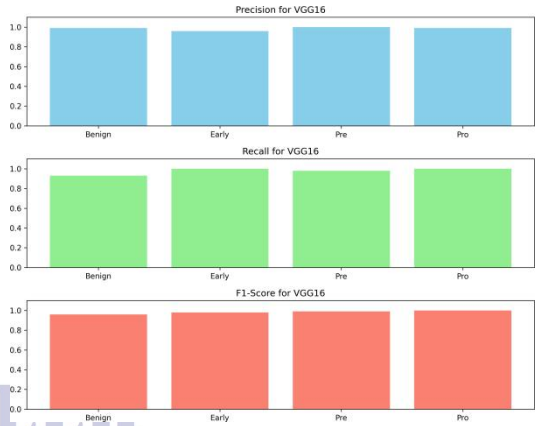

(d) VGG16

Figure 4: Per-class performance metrics (precision, recall, F1-score) for the four CNN models: (a) DenseNet-121, (b) EfficientNet-B3, (c) ResNet-50, and (d) VGG16. All models show strong performance (≥0.90) across Benign, Early Pre-B, Pre-B, and Pro-B classes.

Figure 4a–4d illustrate per-class precision, recall, and F1-score for the four models. All models exhibit strong and balanced performance across the four classes (Benign, Early Pre-B, Pre-B, Pro-B).

Precision, recall, and F1-score values consistently exceed 0.90, with most above 0.95. EfficientNet-B3 achieves the highest and most consistent metrics, with precision, recall, and F1-score at or above 0.98 for all classes, confirming its superior overall accuracy of 98.57%. VGG16 follows closely, showing near-identical high values except for slightly lower recall on the Benign class (0.93), reflecting minor misclassifications observed in its confusion matrix. DenseNet-121 and ResNet-50 display marginally lower scores, particularly on the Benign class (precision and F1-score 0.90–0.95 for ResNet-50), consistent with their higher error rates in distinguishing benign hematogones. The uniformly high per-class metrics demonstrate robust discrimination of subtle morphological differences among ALL subtypes and benign cells across all architectures.

3.4 Discussion

The proposed EfficientNet-B3 model achieves the highest accuracy of 98.57%, surpassing all prior studies. The proposed VGG16 follows closely at 98.37%, and DenseNet-121 at 97.76%, placing three of the top four results among the proposed approaches. Even the proposed ResNet-50 (95.92%) remains competitive with mid-to-high-tier prior works.

The closest prior result is 98.00% reported by Bhute et al. using VGG16, followed by 96.07%

(Haque et al., Incept-ResNet) and 95.45% (Sampathila et al., ALL-NET). Other studies range from 70.01% to 92.0%, demonstrating greater variability in performance.

These results establish EfficientNet-B3 as the new state-of-the-art for this four-class ALL subtype classification task, with the proposed transfer learning framework consistently yielding superior or highly competitive performance across architectures.

Figure 5b and 5a compares the classification accuracies of the proposed models with previously published results on comparable acute lymphoblastic leukemia (ALL) blood smear image datasets.

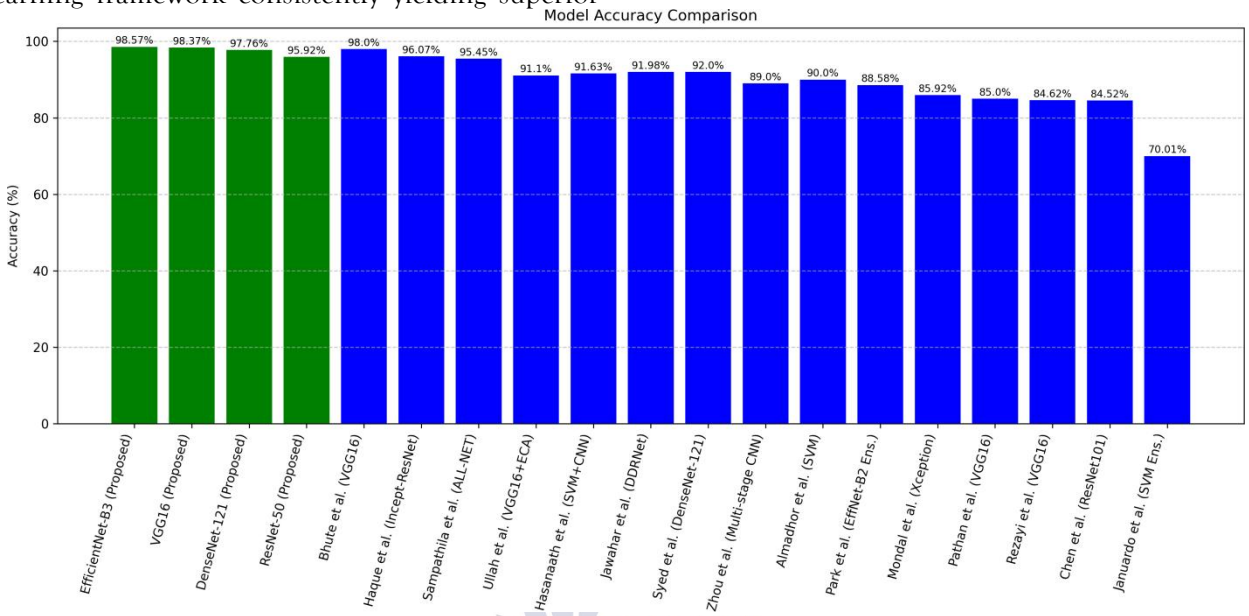

(a) Comparison of test accuracies with prior studies

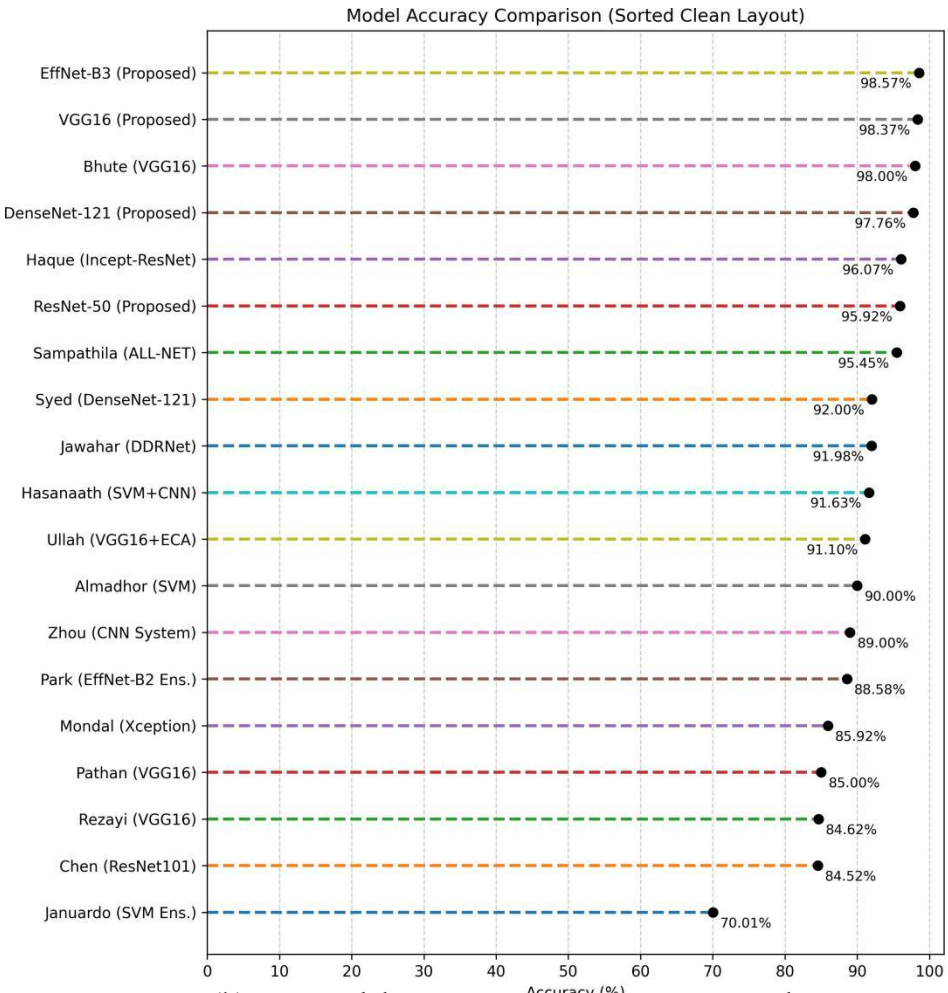

(b) Model Accuracy Comparison Line Chart

Figure 5: Model accuracy comparisons: (a) line chart showing training progression; (b) comparison with prior studies on ALL blood smear datasets.

4 Conclusion

This study presented an automated deep learning–based framework for accurate classification of Acute Lymphoblastic Leukemia (ALL) subtypes using peripheral blood smear images. This method worked extremely well in four clinically important groups: Benign, Early Pre-B, Pre-B, and Pro-B. It did this by using four sophisticated convolutional neural network architectures: EfficientNet-B3, VGG16, DenseNet-121, and ResNet-50. The models that were examined had the best overall performance. EfficientNet-B3 had a test accuracy of 98.57%, which means it was virtually perfect in terms of precision, recall, and F1-scores for all classes. This shows that it is strong and effective in telling the difference between fine-grained leukemia subtypes. The suggested method works extremely well because it uses a well planned preparation and training plan that includes image standardization, normalization, enhancement using HSV-based lymphoblasts, data augmentation, and class-weighted learning to fix the imbalance in the dataset. The models used a two-stage transfer learning methodology, first using generic visual representations from ImageNet, followed by the customization of these features to align with the unique structural patterns seen in blood smear pictures. Comparative studies showed that VGG16 and DenseNet-121 did well, even if deeper designs like ResNet-50 were more badly impacted by class imbalance, especially when it came to sorting minority classes. The suggested technique surpasses several previously reported methods by attaining equivalent or superior accuracy without

the need of cumbersome group procedures. The successful integration of the top-performing model into a

web-based interface demonstrates the practical applicability of our work. With this connection, it's easy to make quick, accurate, and user-friendly predictions for all subtypes. The results suggest that automated deep learning analysis of peripheral blood smear images might assist physicians and laboratory personnel in making better informed decisions, decreasing diagnostic variability, and enabling precise clinical assessments promptly.

References

[1] Pathan, M. S., Bidve, V., Bhapkar, H., Dhotre, P., & Singh, V. B. P. (2023). Leukemia detection system using convolutional neural networks by means of microscopic pictures. *Indonesian Journal of Electrical Engineering and Computer Science*, 31(3), 1616–1623.

[2] Haque, R., Al Sakib, A., Hossain, M. F., Islam, F., Aziz, F. I., Ahmed, M. R., Kannan, S., Rohan, A., & Hasan, M. J. (2024). Advancing early leukemia diagnostics: A comprehensive study incorporating image processing and transfer learning. *BioMedInformatics*, 4, 966–991.

[3] Bhute, A., et al. (2023). Acute lymphoblastic leukemia detection and classification using an ensemble of classifiers and pre-trained convolutional neural networks. *International Journal of Intelligent Systems and Applications in Engineering*, 12(1), 571–580.

[4] Ullah, M. Z., et al. (2021). An attention-based convolutional neural network for acute lymphoblastic leukemia classification. *Applied Sciences*, 11(22), 10662.

[5] Sampathila, N., et al. (2022). Customized deep learning classifier for detection of acute lymphoblastic leukemia using blood smear images. *Healthcare*, 10(10), 1812.

[6] Mondal, C., et al. (2021). Ensemble of convolutional neural networks to diagnose acute lymphoblastic leukemia from microscopic images. *Informatics in Medicine Unlocked*, 27, 100794.

[7] Rezayi, S., et al. (2021). Timely diagnosis of acute lymphoblastic leukemia using artificial intelligence-oriented deep learning methods. *Computational Intelligence and Neuroscience*, 2021, 5478157.

[8] Syed, N., et al. (2025). Novel hierarchical deep learning models predict type of leukemia from whole-slide microscopic images of peripheral blood. *Journal of Medical Artificial Intelligence*, 8(5), 1–14.

[9] Zhou, M., et al. (2021). Development and evaluation of a leukemia diagnosis system using deep learning in real clinical scenarios. *Frontiers in Pediatrics*, 9, 693676.

[10] Almadhor, A., et al. (2022). An efficient computer vision-based approach for acute lymphoblastic leukemia prediction. *Frontiers in Computational Neuroscience*, 16, 1083649.

[11] Aria, M., et al. (2021). Acute lymphoblastic leukemia (ALL) image dataset. Kaggle. 10.34740/KAGGLE/DSV/2175623

[12] Park, S., et al. (2024). Deep learning model for differentiating acute myeloid and lymphoblastic leukemia in peripheral blood cell images. Digital Health, 10, 20552076241258079.

[13] Chen, Y.-M., et al. (2021). Classifying microscopic images as acute lymphoblastic leukemia by ResNet ensemble model and Taguchi method. BMC Bioinformatics, 22(Suppl. 5), 615.

[14] Jawahar, M., et al. (2024). An attention-based deep learning model for acute lymphoblastic leukemia classification. Scientific Reports, 14, 17447.

[15] Januardo, B., et al. (2024). Analysis of ensemble majority voting approach for acute lymphoblastic leukemia detection. Procedia Computer Science, 245, 963–970.

[16] Hasanaath, A. A., et al. (2024). Acute lymphoblastic leukemia detection using

ensemble features from multiple deep CNN models. Electronic Research Archive, 32(4), 2407–2423.

[17] Raza, Ali, et al. iAFP-ET: A robust approach for accurate identification of antifungal peptides using extra tree classifier and multi-view fusion. Tech. Rep.

[18] Shamas, Muneeba, et al. "Classification of pulmonary diseases from chest radiographs using deep transfer learning." PloS one 20.3 (2025): e0316929.

[19] Ghulam, Ali, et al. "ACP-2DCNN: Deep learning-based model for improving prediction of anticancer peptides using two-dimensional convolutional neural network." Chemometrics and Intelligent Laboratory Systems 226 (2022): 104589.

[20] Raza, Ali, et al. "AIPs-SnTCN: Predicting anti-inflammatory peptides using fastText and transformer encoder-based hybrid word embedding with self-normalized temporal convolutional networks." Journal of chemical information and modeling 63.21 (2023): 6537-6554.

[21] Ahmad, Ashfaq, et al. "Deep-AntiFP: Prediction of antifungal peptides using distanct

[22] multi-informative features incorporating with deep neural networks." Chemometrics and Intelligent Laboratory Systems 208 (2021): 104214.

[23] Ahmad, Ashfaq, et al. "iAFPs-EnC-GA: identifying antifungal peptides using sequential and evolutionary descriptors based multi-information fusion and ensemble learning approach." Chemometrics and Intelligent Laboratory Systems 222 (2022): 104516.

[24] Ahmad, Ashfaq, et al. "Identification of antioxidant proteins using a discriminative intelligent model of k-space amino acid pairs based descriptors incorporating with ensemble feature selection." Biocybernetics and Biomedical Engineering 42.2 (2022): 727-735.